Gridded Parasitic Patch Stacked Microstrip Antenna With Beam Shift Capability for 60 GHz Band

Bondarik, Alexander; Sjöberg, Daniel

2014

CODEN:LUTEDX/(TEAT-7233)/1-19/(2014)

Gridded Parasitic Patch Stacked Microstrip Antenna With Beam Shift Capability for 60 GHz Band

Alexander Bondarik and Daniel Sjöberg

Electromagnetic Theory
Department of Electrical and Information Technology
Lund University
Sweden

Alexander Bondarik and Daniel Sjöberg
{Alexander.Bondarik, Daniel.Sjoberg}@eit.lth.se

Department of Electrical and Information Technology
Electromagnetic Theory
Lund University
P.O. Box 118
SE-221 00 Lund
Sweden

Editor: Gerhard Kristensson

Abstract

A microstrip antenna design is introduced in which a rectangular microstrip patch is coupled electromagnetically with a gridded rectangular patch placed above. The gridded patch consists of nine identical rectangular parts separated by a distance which is much smaller than a free space wavelength for a central frequency. The antenna is designed to operate in the 60 GHz band and is fabricated on a conventional PTFE (polytetrafluoroethylene) thin substrate. The antenna return loss bandwidth is comparable to a single parasitic patch aperture coupled antenna, while the proposed antenna gain is higher. Measurement results are in good agreement with simulation. Measured 10 dB return loss bandwidth is from 54 GHz up to 67 GHz. It fully covers the unlicensed band around 60 GHz. The measured antenna realized gain at 60 GHz is close to 8 dB, while the simulated antenna radiation efficiency is 85%. A simple beam shifting method is possible for this antenna structure by connecting adjacent outside parts in the gridded patch. The designed antenna is suitable for a high speed wireless communication system in particular for a user terminal in a fifth generation (5G) cellular network.

1 Introduction

The last decade has seen a heightened interest in the unlicensed frequency band around 60 GHz. Wide, globally available bandwidth and high propagation attenuation allow for numerous applications requiring multi-Gb/s data wireless communication on a short range [6, 17, 23].

The antenna is among the critical elements for a wireless system. It should have a wide bandwidth characteristic to take advantage of the 60 GHz frequency band. For a majority of systems a 7 GHz 10 dB return loss bandwidth is specified. However, for a global usage the antenna should be able to operate from 55 GHz up to 67 GHz, *i.e.*, cover 12 GHz bandwidth [23]. To overcome the propagation attenuation the antenna should have a high efficiency and a high gain. The latter specification implies a sharp antenna beam shape and therefore a beam steering is a requirement for some applications. The beam shift technique should preferably be simple and cost-effective [6]. Another important issue is antenna robustness and ease of integration with other components inside a wireless system. It means that the antenna should be compact and fabricated using conventional techniques [15, pp. 295–348]. Antenna packaging techniques have certain restrictions on substrate material and substrate thickness. Usually there exists a limit in substrate height [14]. Some applications require antenna integration in portable terminals and clothing [3], therefore antenna should be conformal and flexible, which is much easier to achieve with thin substrate.

One of the possible solutions is a patch antenna. However a classical design with a single metal patch above a ground plane cannot satisfy the bandwidth requirement and additional techniques need to be used to enlarge this characteristic. Microstrip antenna structures with multiple resonances have proven to increase operational bandwidth and antenna gain significantly. Designs for 60 GHz are reported

in several papers. An aperture coupled patch antenna is described in [12]. The antenna uses an aperture and a patch as two coupled resonators. As a result 7 GHz bandwidth and 7 dB gain at 60 GHz has been achieved. In [7] a parasitic patch is placed above a probe fed microstrip patch. The combination of two coupled patches gives about 9 GHz bandwidth and about 5 dB gain at 60 GHz. An aperture coupled two patches stacked design is presented in [24]. The features for this antenna are a differential feeding scheme and an H-shape aperture. Reported return loss bandwidth is from 50 GHz to 78 GHz, but the antenna gain has significant drops inside the mentioned band. A microstrip antenna stacked design is presented in [18]. The antenna consists of a probe fed patch and two layers of parasitic patches, four patches in each layer. Due to the large radiating aperture the antenna has a large gain, 11 dB. The return loss bandwidth is about 2 GHz. In [2] an aperture coupled stacked microstrip antenna has four parasitic patches on a top layer. The antenna has 10 GHz bandwidth and 6 dB gain at 60 GHz.

In the current paper a novel aperture coupled microstrip antenna stacked design is proposed. The traditional design introduced in [21] and further investigated carefully in [4, 19, 20, 22] is modified using a gridded structure for the parasitic microstrip patch, instead of a single parasitic patch. The parasitic patch design concept is similar to the gap-coupled rectangular microstrip antennas reported in [9, 10] and [11, pp. 171–203]. The antenna proposed in this paper has nine parasitic patches arranged in a grid and aperture coupling feeding, whereas five parasitic patches and probe feeding were used in [11, pp. 171–203]. In this paper, we explain our design procedure, and make a detailed comparison between our concept and two similar concepts. The first uses a single parasitic patch, whereas the second uses five gap-coupled patches. All three antenna concepts are optimized for 60 GHz band. It is shown that the gridded parasitic patch antenna has the highest gain for the smallest antenna aperture. Compared to the antennas reported in [2, 7, 12, 18, 24] the proposed antenna has improved return loss characteristics in combination with high gain. Moreover, the gridded structure of the parasitic patch can be used for a simple beam shift realization by implementing shorting strips, with just slight decrease in bandwidth and gain. The antenna has high simulated efficiency. The fabrication is relatively simple and uses standard commercial processes. The gridded parasitic patch antenna can be used in a 5G network user terminal where a small thickness, high directivity and beamforming are an issue [1].

The paper is organized as follows. The design of the gridded parasitic patch stacked microstrip antenna is presented in Section 2. In Section 3 alternative antenna designs and their detailed comparison is described. Section 4 contains the parameter study for the proposed antenna. A measurement setup together with the simulated and measured results of the test structure is presented in Section 5. A beam shift realized by connecting some of the parasitic patches is presented in Section 6. Conclusions are made in Section 7.

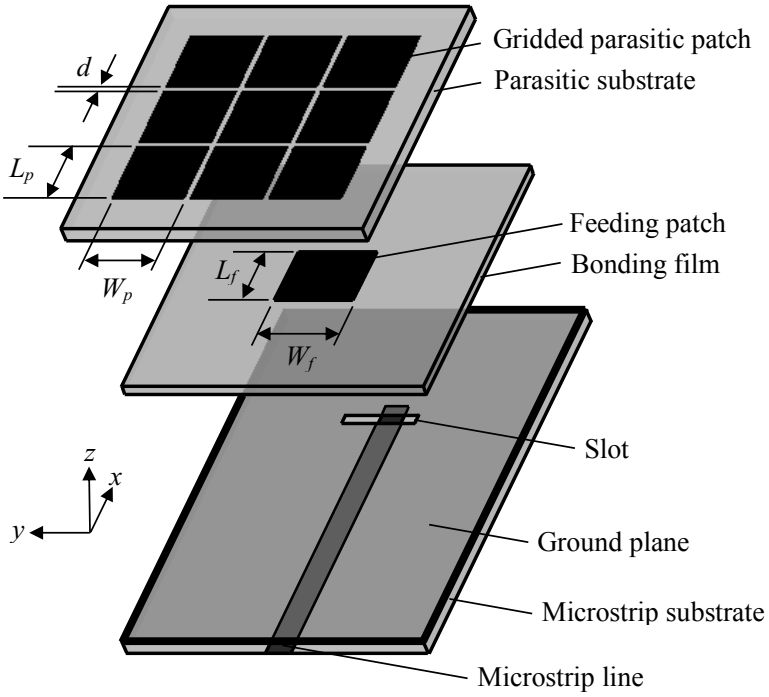

Figure 1: Geometry of the aperture coupled stacked microstrip antenna with gridded parasitic patch.

2 Antenna design

The proposed antenna geometry is shown in Fig. 1. In Table 1 the antenna design parameters are listed. A PTFE (polytetrafluoroethylene) substrate and a bonding film are used to form a three-layer structure. The permittivity for both materials has close values. The fabrication procedure is conventional and not complicated. On the bottom there is a microstrip line that feeds a single rectangular patch ("feeding patch") using aperture coupling through a slot in the ground plane. The bonding film acts as a substrate for the feeding patch. The thickness of the bonding film is small, compared to the substrate thickness, and ensures a strong coupling to the microstrip line. On the top, there is a gridded parasitic patch formed by nine identical rectangular parts. The gridded patch is coupled electromagnetically to the feeding patch without vias implementation. The separation between the rectangular parts in the gridded patch is at the fabrication limit. The idea is to keep a strong coupling between different parts. Aperture coupling in the ground plane allows exciting the feed patch symmetrically. The latter feature has an influence on radiation pattern symmetry.

All the antenna design parameters affect the antenna characteristics. The substrate and bonding film parameters were considered as fixed to keep the fabrication process conventional. This gave the entry point to the design. On the first stage the microstrip line width was adjusted to have $50\,\Omega$ impedance. On the second stage, in the absence of the parasitic patch, the ground plane aperture size and feeding

Description	Value
substrate Taconic TLY-5	$\epsilon_r = 2.2$, $\tan\delta = 0.0009$
parasitic substrate thickness	0.127 mm
microstrip substrate thickness	0.127 mm
bonding film Arlon CuClad 6700	$\epsilon_r = 2.35$, $\tan\delta = 0.0025$
bonding film thickness	0.0762 mm
microstrip line width	0.375 mm
microstrip line stub, S	0.50 mm
slot length, L_s	0.20 mm
slot width, W_s	0.85 mm
feeding patch length, L_f	1.10 mm
feeding patch width, W_f	1.29 mm
parasitic patch length, L_p	1.156 mm
parasitic patch width, W_p	1.20 mm
parasitic patches separation, d	0.10 mm

Table 1: Stacked microstrip antenna design parameters.

patch size were optimized to have a good coupling between the microstrip line and the feeding patch. The feeding patch length and width initial values were chosen to be around half of a wavelength in the substrate. On the third stage the gridded parasitic patch was placed above the feeding patch. The separation between the rectangular parts in the gridded patch was set to a fixed value of 0.1 mm, which is the limit for the manufacturing process. On this stage it should be recognized that the ground plane aperture size, feeding patch size, and gridded patch size are strongly related to each other. The gridded patch size was varied in a wide range to find a broadband solution for the antenna. At the same time the other parameters were varied in a narrow range, around the existing after the second design stage values. In order to have a margin and to mitigate the mismatch losses for the antenna design with beam shift, the optimization goal for the return loss was set to 20 dB for frequencies 57 GHz–63 GHz. Optimization was performed using CST Microwave Studio software. The fabricated antenna sample is shown in Fig. 2. The total antenna substrate thickness is 0.33 mm, which is about $0.066\lambda_0$ expressed in the free space wavelength at 60 GHz, and about $0.1\lambda_0$ electrical length if the substrate permittivity is taken into account. The substrate thickness above a ground plane is $0.04\lambda_0$, which is about $0.06\lambda_0$ electrical length.

3 Antenna comparison

In this section we make a detailed comparison of the proposed antenna to published antenna structures. In particular it is important to weigh the gridded parasitic patch to the well-studied and widely used single parasitic patch. In [20] 69% measured 10 dB return loss bandwidth is reported. To achieve such a wide bandwidth a com-

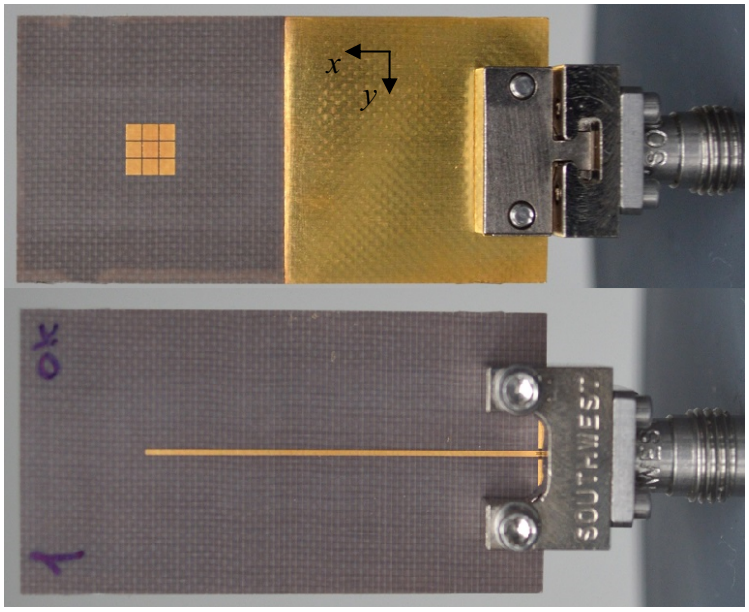

Figure 2: Front and backside photographs of the fabricated antenna with end launch connector.

bination of moderate ($\epsilon_r = 2.2$) and low ($\epsilon_r = 1.07$) dielectric constant substrates is used, moreover a superstrate layer ($\epsilon_r = 2.53$) is used. The total substrate thickness for the dielectric above a ground plane is about $0.2\lambda_0$ for 7 GHz central frequency, the corresponding electrical length is about $0.25\lambda_0$. For 60 GHz central frequency the scaled substrate thickness would be 1 mm, and it can be a considerable fraction of thickness for a user terminal, like mobile phone with less than 10 mm thickness.

In the presented work the intention was to use a non-complicated fabrication process avoiding thick multi-layer substrates and air cavities that might emulate the foam substrate used in [20]. The substrate structure and parameters for the aperture coupled single parasitic patch antenna design are shown in Fig. 1 and listed in Table 1. During the parametric study it was found that to match the antenna at 60 GHz the parasitic patch width should be several times more than length. For 20 dB return loss optimized parasitic patch width is 7 mm, the parasitic patch length is 1.38 mm. In Fig. 3 is shown simulated reflection coefficient for the single parasitic patch antenna (dashed line). In Table 2 the antenna design parameters are listed. Even though the single parasitic patch antenna has acceptable return loss characteristic, it is considered as impractical due to the big ratio between radiating patch width and length, which is more than 5. The common suggestion is to keep the ratio less than 2 in order to avoid the additional modes excitation [5]. This means that it is impossible to design a reliable aperture coupled single parasitic patch antenna for the chosen substrate. It has been noticed that the way to keep the parasitic patch width comparable to length is to increase the parasitic substrate thickness. For example, for the parasitic substrate thickness 0.43 mm, the optimized antenna has the slot and the feeding patch dimensions same as in Table 1, with the

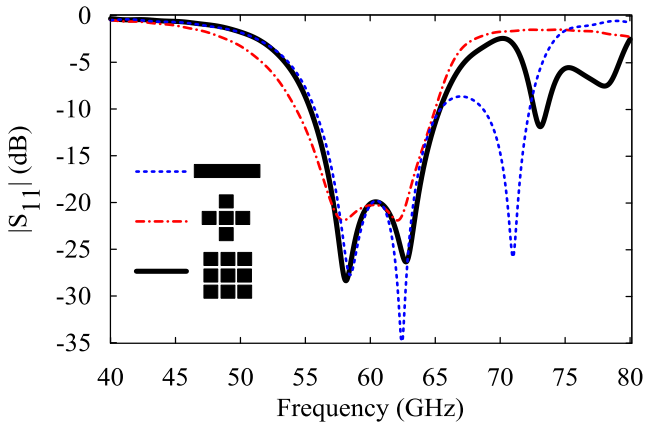

Figure 3: Simulated reflection coefficient of the single parasitic patch antenna (design parameters see in Table 2), five gap-coupled parasitic patches antenna (design parameters see in Table 2), and gridded parasitic patch antenna (design parameters see in Table 1).

Parameter	Single parasitic	Five parasitic
S	0.65 mm	0.69 mm
L_s	0.19 mm	0.24 mm
W_s	0.89 mm	0.85 mm
L_f	1.15 mm	0.87 mm
W_f	1.30 mm	0.83 mm
L_p	1.38 mm	1.35 mm
W_p	7.00 mm	1.41 mm
d		0.20 mm

Table 2: Design parameters for antenna comparison.

parasitic patch width 1.4 mm and length 1.2 mm.

The other way to match the single parasitic patch antenna on a substrate of given thickness is to add additional parasitic patches close to the main patch on the antenna top layer. The alternative interpretation is the division of the wide parasitic patch into close coupled patches. This approach is described in [9, 10] and [11, pp. 171–203]. In case when four parasitic patches are placed along to a single patch sides, the parasitic patches geometry is forming a structure similar to a plus sign. A stacked antenna structure with this parasitic patches arrangement is studied in [11, pp. 171–203], where a probe feeding is used to design the antenna. However, we have not found a previous use of an aperture coupling feeding for this antenna. In Fig. 3 is shown simulated reflection coefficient for the five parasitic patches antenna (dot-and-dash line). In Table 2 the antenna design parameters are listed. The total antenna width is 4.63 mm, which is 1.5 times less than for the single parasitic antenna.

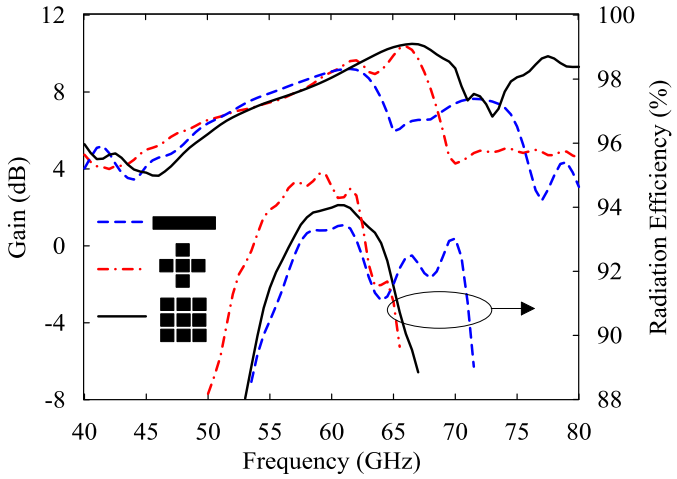

Figure 4: Simulated gain and radiation efficiency of the single parasitic patch antenna, five gap-coupled parasitic patches antenna, and gridded parasitic patch antenna.

The natural development for the five parasitic patches antenna would be adding four more parasitic patches forming a gridded structure. This design does not require the additional increase in antenna aperture length and width. By doing this we introduce a novel aperture coupled stacked microstrip antenna with gridded patch. The design parameters for this antenna were presented in the previous chapter. The total antenna width is 3.8 mm, which is 1.8 times less than for the single parasitic antenna and 1.2 times less than five parasitic patches antenna. The simulated reflection coefficient is shown in Fig. 3 (solid line).

Comparing the reflection coefficient for the three antennas in Fig. 3 one can notice that all of them have approximately the same 20 dB reflection coefficient bandwidth, about 6.2 GHz. The antennas are based on the same substrate and three layer structure. The difference is in the parasitic radiator geometry, however the parasitic patch length is approximately the same for all the antennas.

In Fig. 4 is shown the proposed antenna simulated maximum antenna gain and radiation efficiency compared with two alternative antenna designs. In Fig. 5 is shown normalized radiation patterns for the three antennas. The ground plane size is 10 mm by 10 mm for all antennas. The gridded parasitic patch antenna and five parasitic patches antenna have almost the same maximum gain 10.5 dB, and similar radiation patterns. However, the former antenna has the widest 3 dB gain bandwidth, about 17 GHz, compared to the latter antenna, about 14 GHz. Due to the wide radiating patch, the single parasitic patch antenna has quite high gain, about 9 dB. However, the radiation pattern is pretty much asymmetrical and is oblong in the E-plane. The peak radiation efficiency is the highest for five gap-coupled parasitic patches antenna. However the difference with the proposed antenna is only 1 percentage point.

To conclude the comparison, the proposed aperture coupled gridded parasitic patch stacked microstrip antenna structure has improved radiation characteristic

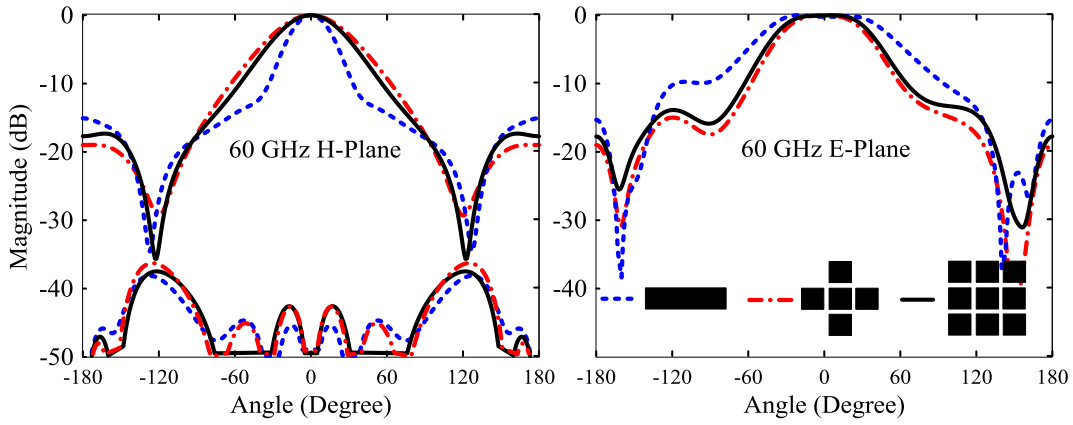

Figure 5: Simulated normalized radiation patterns in the H-plane and in the E-plane of the single parasitic patch antenna, five gap-coupled parasitic patches antenna, and gridded parasitic patch antenna. Co-polarization and cross-polarization patterns are presented. In the E-plane the cross-polarization level is out of the scale. Patterns are given for the central frequency 60 GHz.

compared to similar considered stacked microstrip antenna configurations. It has the widest gain bandwidth and the smallest radiating aperture.

4 Parameter study

All the parameters listed in Table 1 affect the antenna characteristics. The variation in slot size, feeding patch size, parasitic patch size, and substrate thickness has similar effect as for the aperture coupled stacked antenna with single parasitic patch, which is carefully investigated in [4] and [20]. In this section a parameter study for the gridded parasitic patch antenna is focused on the influence of the separation d between adjacent parasitic patches in the grid. In Fig. 6 is shown the simulation result for different separation values. The frequency variation is from 50 GHz to 70 GHz. The optimized separation is $d = 0.1$ mm, and the variation from this value results in impedance mismatch. The effect is to reduce the coupling between feeding and gridded patch destroying the second tight loop typical for three resonances aperture coupled stacked structure [20]. The parasitic patches resonance behavior can be modelled as a resonator with equivalent impedance. Based on this model the mismatch presented in Fig. 6 can be explained by change in the equivalent reactance when the distance between parasitic patches is changed. Indeed, the impedance loci turn counterclockwise in Fig. 6(a) when decreasing the equivalent reactance and turn clockwise in Fig. 6(b) when increasing the equivalent reactance.

The antenna impedance mismatch due to the change in separation d can be partially compensated for by changing the substrate thickness h between the feeding patch and parasitic patches. In Fig. 7 is shown the simulation result for decreased d, and for increased d. Further optimization can be made using parasitic patches size

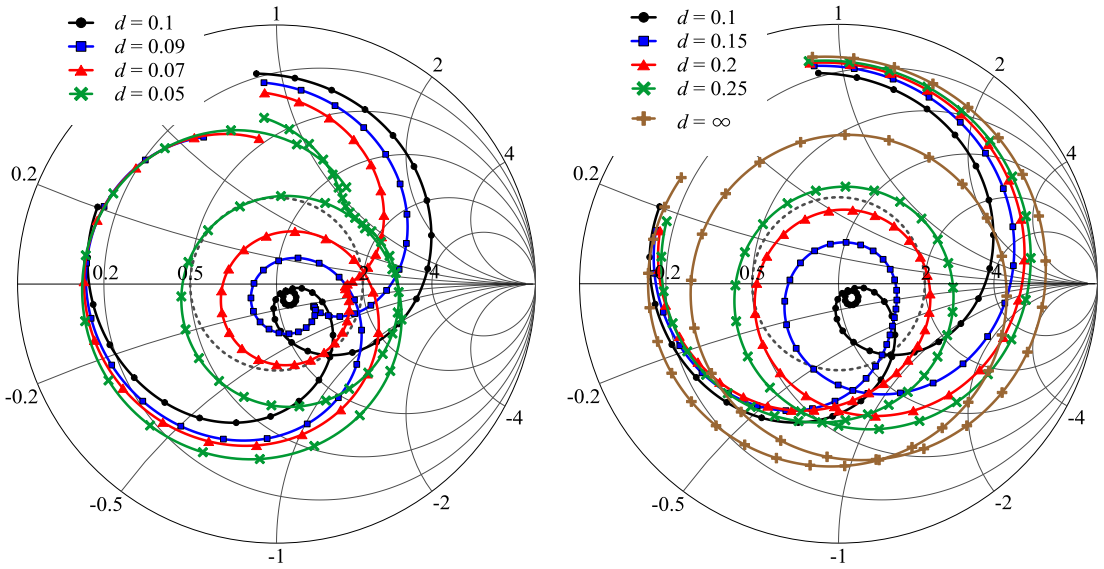

Figure 6: Simulated impedance loci for the gridded parasitic patch antenna as a function of the separation d (in mm) between adjacent patches in the grid. (a) Separation is decreased. (b) Separation is increased.

optimization together with additional slight change in the substrate thickness h. As an example it can be mentioned the single parasitic patch antenna described in the previous section. This corresponds to the case when either d is infinitely large or $d = 0\,\text{mm}$. Another example is for $d = 0.15\,\text{mm}$. Optimized design parameters are as following. Parasitic patches substrate thickness is $0.177\,\text{mm}$. Parasitic patches length is $1.1\,\text{mm}$ and width is $0.9\,\text{mm}$. All remaining parameters are kept as in Table 1. For 20 dB level the optimized antenna bandwidth is about $7.65\,\text{GHz}$, which is about $1\,\text{GHz}$ less than for optimized antenna with $d = 0.1\,\text{mm}$.

5 Measurement results

The aperture coupled gridded parasitic patch stacked microstrip antenna parameters were measured using a $67\,\text{GHz}$ Agilent E836A PNA network analyzer. The antenna was fed through a $1.85\,\text{mm}$ end launch connector from Southwest Microwave company. To be able to attach the connector the fabricated antenna samples substrate was made large enough. The sample size was $40\,\text{mm}$ by $20\,\text{mm}$. A part of the substrate close to the connector was removed to expose the ground plane and ensure a good contact for the connector. The remaining substrate size is $20\,\text{mm}$ by $20\,\text{mm}$. To validate the antenna measurements a 3D connector model was developed in CST. Moreover, the microstrip line area that is in touch with the connector was optimized to have a tapered form and it has metal pads at both sides to be matched to the connector and to have a good contact with the connector body. The following

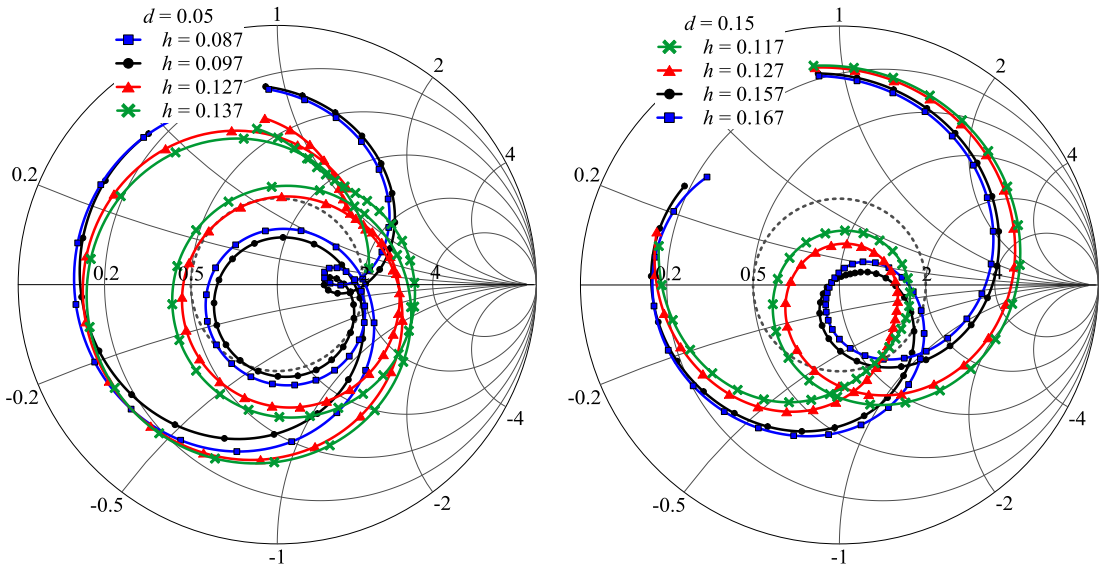

Figure 7: Simulated impedance loci for the gridded parasitic patch antenna as a function of the substrate height h (in mm) between feeding and parasitic patches. (a) For $d = 0.05\,\text{mm}$ optimal is $h = 0.097\,\text{mm}$. (b) For $d = 0.15\,\text{mm}$ optimal is $h = 0.157\,\text{mm}$.

measurement results are compared to a simulation that includes the antenna and the connector as a single system. To investigate the connector influence, simulated results for the antenna without connector are presented as well. These results are not the same as presented in Section 2 due to the different substrate size in simulation. For the various antenna type investigation the substrate size was 10 mm by 10 mm. As will be shown the return loss is slightly different, however the radiation pattern has considerable differences for larger substrate.

5.1 Reflection Coefficient

The measured and simulated reflection coefficient for the antenna is shown in Fig. 8. It can be seen from the graph that the measured 10 dB return loss range is approximately from 54 GHz up to 67 GHz. It is about 22% compared to the 60 GHz central frequency. For the communication band from 57 GHz to 64 GHz the return loss is less than $-15\,\text{dB}$. The measured result is close to both simulated results for the antenna with and without connector. This confirms the connector reliability and small influence on the antenna return loss. Further post processing, like connector de-embedding, may amend the measured return loss.

5.2 Radiation patterns

The antenna radiation patterns and gain measurements were performed in a regular office room with scattering environment, the approximate room size is 10 m by 7 m

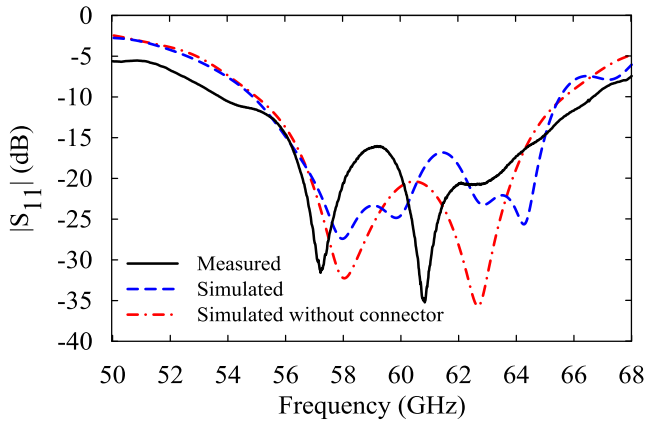

Figure 8: Measured and simulated reflection coefficient of the antenna.

by 2.5 m. The setup was placed approximately in the middle of the room and was organized to minimize the influence of the scattering in the given room. A setup photo is shown in Fig. 9. The antenna under test (AUT) was placed on a rotating platform. A standard horn antenna, connected to a low-noise amplifier (LNA), was used to register the signal. Measured and simulated normalized radiation patterns for 57 GHz, 60 GHz, and 64 GHz are shown in Fig. 10. Co-polarization and cross-polarization components in H-plane (yz plane) and E-plane (xz plane) are presented. In the E-plane the simulated cross-polarization level is out of the scale for the graphs. For comparison, simulated results for the antenna without connector are presented. Measured patterns are close to simulated patterns. For the main beam, in the range between $-90°$ and $90°$, the patterns are almost coinciding. Small differences can be observed for the antenna back radiation.

The measured H-plane patterns different levels for the back radiation for negative and positive angles due to the fact that the setup itself is not symmetrical. There was the network analyzer on one of the sides, and the distances to the walls were not identical. However, the measured maximum back radiation level at $\pm 180°$ for 60 GHz and 64 GHz coincides with simulation within 2 dB, for 57 GHz the measured level is lower, this might be the measurement error. Measured results are in better agreement with the simulation that includes connector. This gives reason to state that for the antenna itself, without the connector influence, the back radiation level is close to the simulated results without connector, which is about -20 dB for 57 GHz and 60 GHz, for 64 GHz the level is close to -30 dB. The measured cross-polarization component is less than -25 dB for considered frequencies.

The E-plane co-polarization radiation patterns have wider asymmetrical main beam compared to the H-plane patterns, and the patterns have ripples for all angles. The measured cross-polarization level is about -30 dB for the frequencies presented in Fig. 10. For the gridded parasitic patch antenna there is an explicit local peak in the E-plane at the angles from about $90°$ to $110°$. This peak disappears for the simulation without connector.

Moreover, the back radiation level for this simulation is about 10 dB lower com-

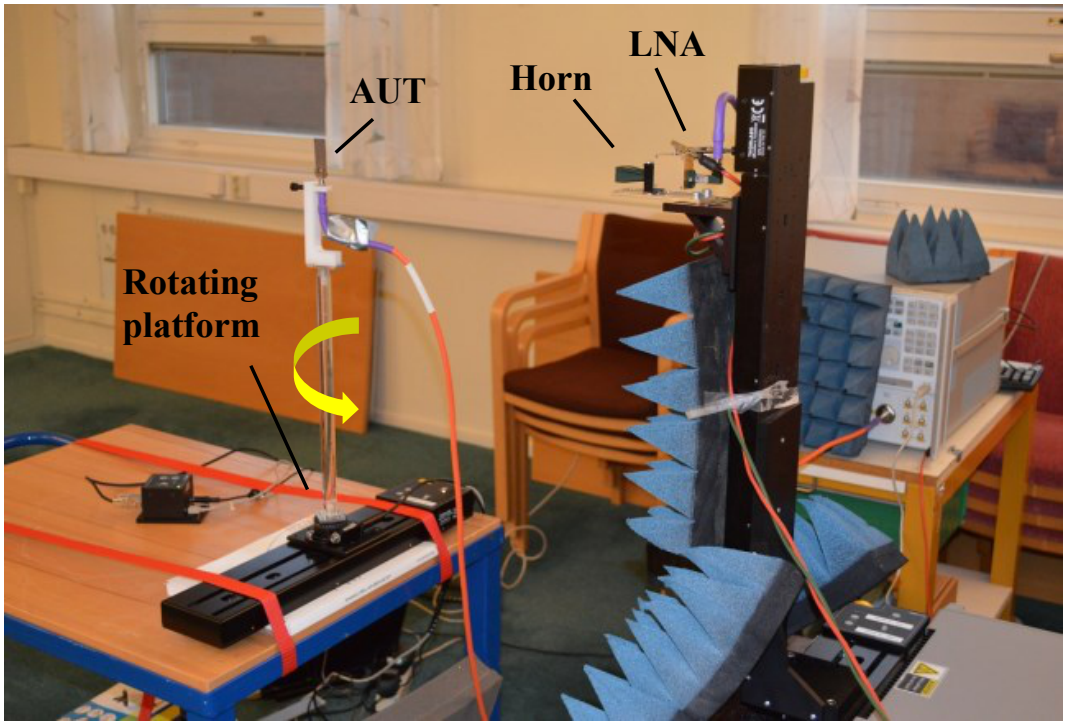

Figure 9: Radiation pattern measurement setup.

pared to the measured pattern. The explanation for the described effect is the presence of radiation along the substrate (xy plane). In Fig. 11 is shown the simulated top surface electric field distribution for the antenna without the connector. The wave reflected from the connector causes the mentioned local peak around 90°. It can be observed from Fig. 11 that the radiation along the substrate is symmetrical with respect to xz plane and asymmetrical with respect to yz plane. This explains the asymmetry in the E-plane radiation pattern even for the simulation without connector. The diffraction of waves radiated along the substrate causes mentioned ripples in the E-plane radiation pattern. The asymmetry in the radiation pattern and ripples decrease for decreased substrate size. Indeed, presented in Fig. 5 E-plane radiation pattern for the gridded parasitic patch is almost symmetrical and without any ripples. In the system design where the antenna should be integrated the substrate size can be much less than that used for measurement with connector. Moreover, it is advantageous to put interfering components in the antenna H-plane. The same rule can be applied for the connector to measure the antenna. However, this introduces additional complications in feeding line bend and length extension. Another solution to improve the radiation pattern symmetry is to use electromagnetic band-gap structures [13] to further constrain the surface waves.

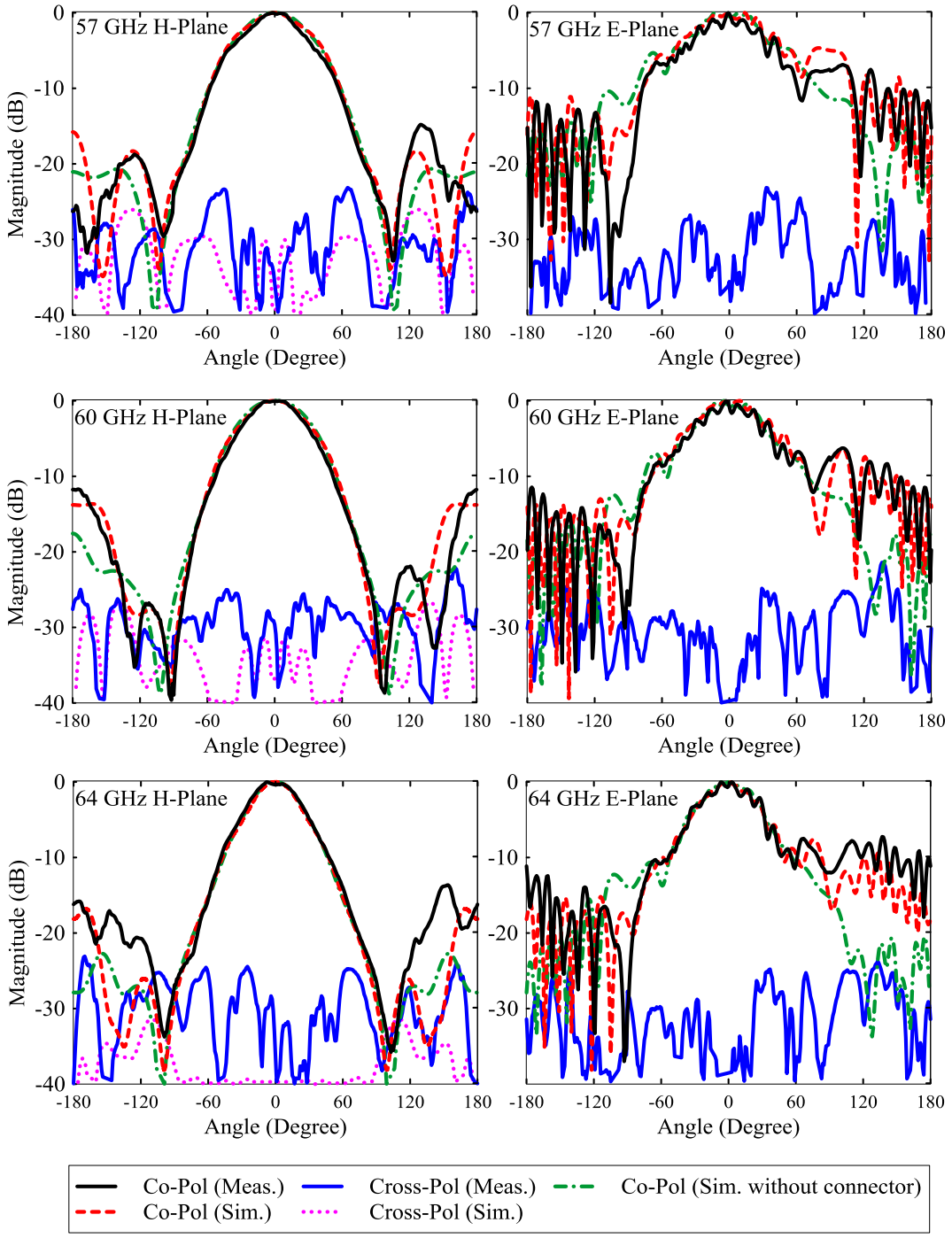

Figure 10: Measured and simulated normalized radiation patterns in the H-plane and in the E-plane of the antenna with end launch connector. Co-polarization and cross-polarization patterns for three frequencies of interest are presented. In the E-plane the simulated cross-polarization level is out of the scale. Simulation results for the antenna without connector are presented as well.

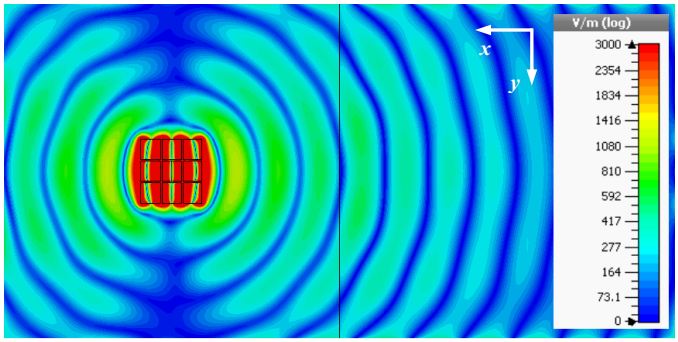

Figure 11: Simulated absolute value of the electric field distribution at 60 GHz, at the top surface of the structure.

5.3 Gain and efficiency

The antenna realized gain was measured based on the gain-transfer method [8]. The AUT was replaced by a standard horn antenna after radiation pattern measurements. Assuming the AUT as transmitting antenna connected to the first port of the network analyzer, the AUT realized gain (or, more precisely, partial realized gain) was calculated using the following equation.

$$G_{\mathrm{AUT,dB}} = 20\log_{10}|S_{21,\mathrm{AUT}}| - 20\log_{10}|S_{21,\mathrm{Horn}}| + G_{\mathrm{Horn,dB}} - \mathrm{TL} \qquad (5.1)$$

Here, $S_{21,\mathrm{AUT}}$ was measured with AUT connected, $S_{21,\mathrm{Horn}}$ was measured with standard horn connected. The term $G_{\mathrm{Horn,dB}}$ is the standard horn gain, available in a data sheet. The term TL is a loss in the coaxial to waveguide transition which was used to connect the standard horn antenna, the loss was estimated as 1 dB. Measured and simulated realized gain is shown in Fig. 12. For comparison, the antenna gain when simulated without connector is also shown. The agreement between measurements and simulation is good. All three curves agree within 2 dB in the frequency range from 57 GHz up to 62 GHz. Maximum measured realized gain is about 9 dB for 66 GHz. At 60 GHz the antenna has about 8 dB realized gain. However, based on the simulation results, the influence of the connector decreases gain bandwidth, and the antenna itself should have wider bandwidth than measured. In the application when the antenna should be integrated with other components some degradation of parameters should be expected.

The radiation efficiency presented in Fig. 12 is obtained from a simulation without the connector. The simulation model considers losses in the substrate and bonding film, metal layers are represented as 18 μm lossy copper. The maximum radiation efficiency for 40 mm by 20 mm sample is about 86% and appears at 57.5 GHz. For 60 GHz the antenna efficiency is about 85%. For 10 mm by 10 mm sample the simulated radiation efficiency is presented in Fig. 4. The maximum value is about 94%.

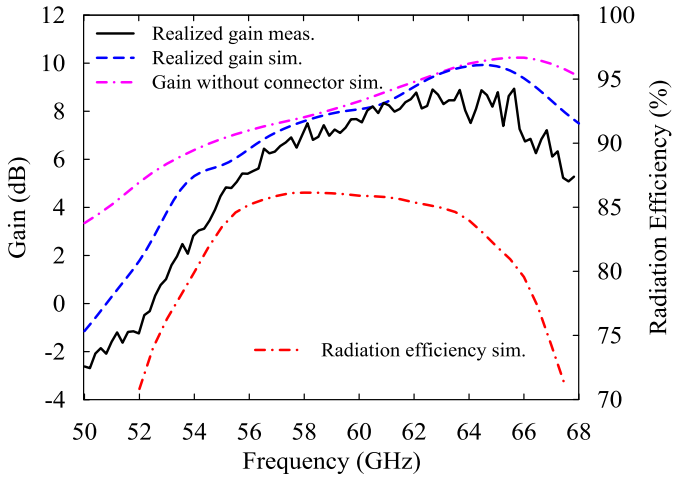

Figure 12: Measured and simulated realized gain of the antenna with connector is compared to the simulated gain of the antenna without connector. Radiation efficiency simulation result for the antenna without connector.

6 Beam shift realization

In this section the example of the simple beam shift realization for the gridded parasitic patch antenna is described. The purpose of this section is to introduce the beam shift principle and to outline thereby the significance of the proposed antenna. The simulated results are presented. Due to the limited space the detailed investigation of the phenomena and experimental results are out of the scope for the current paper.

The proposed beam shift is realized by utilizing the so called ESPAR (Electronically Steerable Parasitic Array Radiator) principle [16]. The ESPAR exhibits a unique phase shifting mechanism where mutual coupling between adjacent radiators feeds the parasitic radiators; and tunable reactive loading at the terminals of the parasitic radiators creates the necessary phase shift, [16]. Usually diode varactors are used to introduce an additional capacitive impedance between parasitic radiators and to change the phase of the radiators excitation. The parasitic element gridded structure has an important advantage. It is possible to realize a radiating structure asymmetry by connecting adjacent patches in the grid. This leads to the antenna beam shift without considerable degradation in return loss and gain. In Fig. 13 is shown the example where three patches are connected by shorting metal pins in the xz plane. The shorting pin width is 0.1 mm. As a result the H-plane antenna beam shift is achieved. Practically this can be accomplished implementing a switch (either on ground plane side or on top layer side) using PIN diodes. Then by opening or closing the switch a beam steering can be achieved. The simulation was performed to check the beam shift capability for the gridded parasitic patch. The ground plane size in the model was 10 mm by 10 mm. Shorting pins implementation change the mutual coupling between the feeding patch and the gridded parasitic patch. This results in the antenna and the feeding line impedance mismatch. The

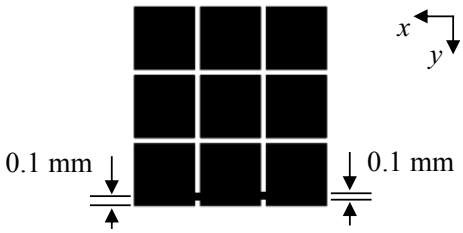

Figure 13: Top view geometry for the gridded parasitic patch with shorting pins enabling the H-plane beam shift. The pin width is 0.1 mm, distance from the pin center to the patch edge is 0.1 mm.

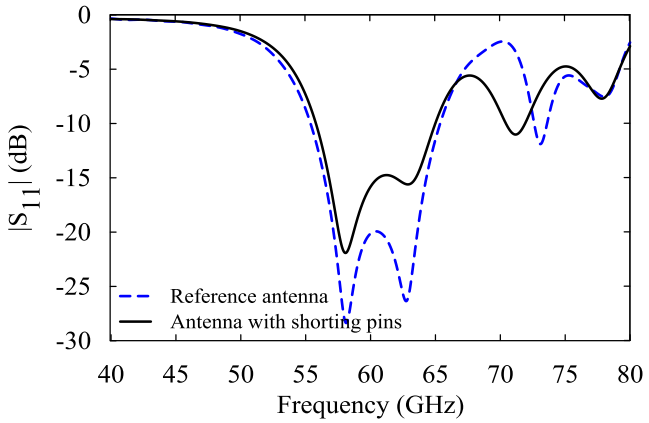

Figure 14: Simulated reflection coefficient for the antenna with beam shift and for the reference antenna without beam shift.

antenna return loss when the adjacent parts are connected is shown in Fig. 14, for the comparison the reference antenna without shorting pins return loss is presented. The antenna with shorting pins 10 dB bandwidth is 9.2 GHz which is slightly less compared to the reference antenna 10 GHz return loss. A low 20 dB return loss level for the reference antenna provides some safety factor in the geometry modification.

Fig. 15 shows the simulated antenna with shorting pins gain radiation patterns compared to the reference antenna radiation patterns at 60 GHz. In the H-plane the antenna with shorting pins has 8° beam shift angle, the maximum gain is 0.6 dB lower than for the reference antenna, the beam width is 62° compared to the 54° reference antenna beam width. In the E-plane there is no beam shift for the antenna with shorting pins, it is still has maximum in the broadside direction, like the reference antenna. The maximum gain difference is 0.8 dB.

Although the antenna with beam shift has some degradation in gain and return loss bandwidth, it is not significant. It confirms that the proposed beam shift method is effective.

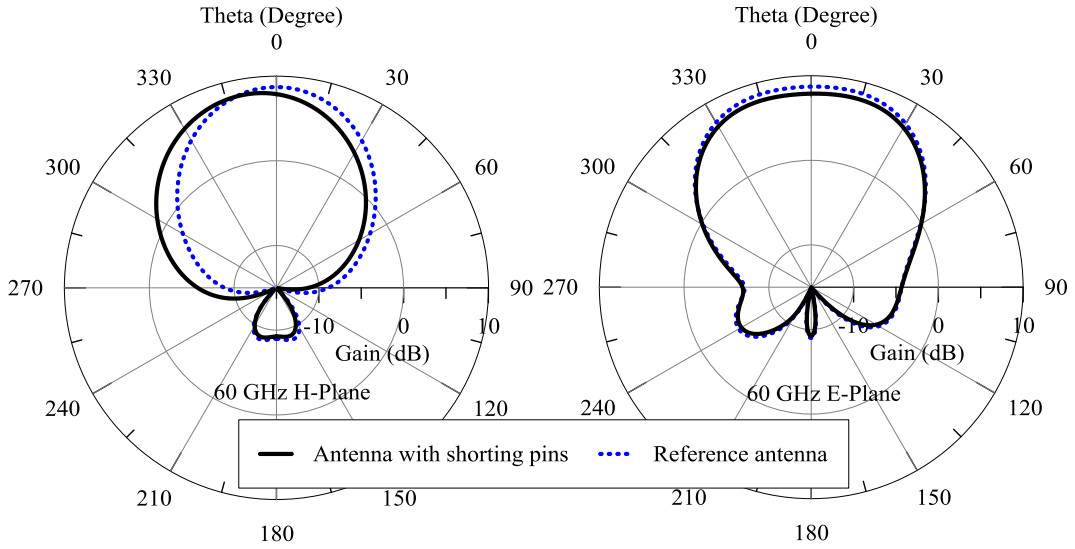

Figure 15: Simulated radiation patterns at 60 GHz for the antenna with beam shift and for the reference antenna without beam shift.

7 Conclusions

A stacked microstrip antenna with novel gridded patch was designed, fabricated, and tested. To validate the measurements a 3D end launch connector model was developed and the influence of the connector was examined. Measured results are very close to the simulated results. The antenna has wide return loss bandwidth that fully covers the unlicensed communication band around 60 GHz. The antenna has high efficiency inside the operational band and wider gain bandwidth compared to the conventional aperture coupled stacked microstrip antenna with single parasitic patch and with five gap coupled parasitic patches. The gridded structure for the proposed antenna can be used to realize a simple beam shift by connecting adjacent patches in the grid. Potentially it is possible to build the antenna array placing proposed antennas such that the separation between edges is the same as in the gridded parasitic structure $d = 0.1$ mm. For this arrangement the distance between single antennas centers is $0.78\lambda_0$. If gridded patches in the array are allowed to overlap between neighbors the distance between feeding patches is about $0.5\lambda_0$. The proposed antenna is suitable for 60 GHz multi-Gb/s data wireless communication systems for the next generation cellular network.

Acknowledgment

The authors would like to thank Mr. Renato Morosin and Mr. Duke Villanueva for the help in the fabrication process, and Mr. Carl Gustafson for the help in measurements.

References

[1] F. Boccardi, R. W. Heath, A. Lozano, T. L. Marzetta, and P. Popovski. Five disruptive technology directions for 5G. *IEEE Commun. Mag.*, **52**(2), 74–80, feb 2014.

[2] A. Bondarik, D. S. Jun, J. M. Kim, and J. H. Yun. Investigation of microstrip antenna array stacked structure realized on LTCC for 60 GHz band. *Microwave and Optical Technology Letters*, **52**(3), 648–652, 2010.

[3] N. Chahat, M. Zhadobov, and R. Sauleau. Wearable textile patch antenna for BAN at 60 GHz. In *Antennas and Propagation (EuCAP), 2013 7th European Conference on*, pages 217–219. IEEE, 2013.

[4] F. Croq and D. M. Pozar. Millimeter-wave design of wide-band aperture-coupled stacked microstrip antennas. *Antennas and Propagation, IEEE Transactions on*, **39**(12), 1770–1776, 1991.

[5] A. Derneryd and A. Lind. Extended analysis of rectangular microstrip resonator antennas. *Antennas and Propagation, IEEE Transactions on*, **27**(6), 846–849, 1979.

[6] N. Guo, R. C. Qiu, S. S. Mo, and K. Takahashi. 60-GHz millimeter-wave radio: Principle, technology, and new results. *EURASIP Journal on Wireless Communications and Networking*, **2007**(1), 48–48, 2007.

[7] W. Hong, A. Goudelev, K.-h. Baek, V. Arkhipenkov, and J. Lee. 24-element antenna-in-package for stationary 60-GHz communication scenarios. *Antennas and Wireless Propagation Letters, IEEE*, **10**, 738–741, 2011.

[8] IEEE standard test procedures for antennas, 2008. IEEE Std 149-1979 (R2008).

[9] G. Kumar and K. C. Gupta. Nonradiating edges and four edges gap-coupled multiple resonator broad-band microstrip antennas. *Antennas and Propagation, IEEE Transactions on*, **33**(2), 173–178, 1985.

[10] G. Kumar and K. P. Ray. Stacked gap-coupled multi-resonator rectangular microstrip antennas. In *Antennas and Propagation Society International Symposium, 2001. IEEE*, volume 3, pages 514–517. IEEE, 2001.

[11] G. Kumar and K. P. Ray. *Broadband microstrip antennas*. Artech House, 2002.

[12] A. E. I. Lamminen, J. Saily, and A. R. Vimpari. 60-GHz patch antennas and arrays on LTCC with embedded-cavity substrates. *Antennas and Propagation, IEEE Transactions on*, **56**(9), 2865–2874, 2008.

[13] A. E. I. Lamminen, A. R. Vimpari, and J. Saily. UC-EBG on LTCC for 60-GHz frequency band antenna applications. *Antennas and Propagation, IEEE Transactions on*, **57**(10), 2904–2912, 2009.

[14] R. Li, G. DeJean, M. Maeng, K. Lim, S. Pinel, M. M. Tentzeris, and J. Laskar. Design of compact stacked-patch antennas in LTCC multilayer packaging modules for wireless applications. *Advanced Packaging, IEEE Transactions on*, **27**(4), 581–589, 2004.

[15] R. Liu, C. Ji, J. J. Mock, J. Y. Chin, T. J. Cui, and D. R. Smith. Broadband ground-plane cloak. *Science*, **323**(5912), 366–369, 2009.

[16] J. J. Luther, S. Ebadi, and X. Gong. A microstrip patch electronically steerable parasitic array radiator (ESPAR) antenna with reactance-tuned coupling and maintained resonance. *Antennas and Propagation, IEEE Transactions on*, **60**(4), 1803–1813, 2012.

[17] B. Schulte, M. Peter, R. Felbecker, W. Keusgen, R. Steffen, H. Schumacher, M. Hellfeld, A. Barghouthi, S. Krone, F. Guderian, G. P. Fettweis, and V. Ziegler. 60 GHz WLAN applications and implementation aspects. *International Journal of Microwave and Wireless Technologies*, **3**(special issue 2), 213–221, April 2011.

[18] T. Seki, N. Honma, K. Nishikawa, and K. Tsunekawa. Millimeter-wave high-efficiency multilayer parasitic microstrip antenna array on teflon substrate. *Microwave Theory and Techniques, IEEE Transactions on*, **53**(6), 2101–2106, 2005.

[19] S. D. Targonski and R. B. Waterhouse. An aperture coupled stacked patch antenna with 50% bandwidth. In *Antennas and Propagation Society International Symposium, 1996. AP-S. Digest*, volume 1, pages 18–21. IEEE, 1996.

[20] S. D. Targonski, R. B. Waterhouse, and D. M. Pozar. Design of wide-band aperture-stacked patch microstrip antennas. *Antennas and Propagation, IEEE Transactions on*, **46**(9), 1245–1251, 1998.

[21] C. H. Tsao, Y. M. Hwang, F. Kilburg, and F. Dietrich. Aperture-coupled patch antennas with wide-bandwidth and dual-polarization capabilities. In *Antennas and Propagation Society International Symposium, 1988. AP-S. Digest*, pages 936–939. IEEE, 1988.

[22] R. B. Waterhouse. Design and performance of large phased arrays of aperture stacked patches. *Antennas and Propagation, IEEE Transactions on*, **49**(2), 292–297, 2001.

[23] J. Wells. Faster than fiber: the future of multi-Gb/s wireless. *IEEE Microw. Mag.*, **10**(3), 104–112, March 2009.

[24] B. Yang, A. Yarovoy, and S. E. Amaldoss. Performance analysis of a novel LTCC UWB 60 GHz semi-shielded aperture stacked patch antenna with differential feeding. In *Antennas and Propagation (EUCAP), Proceedings of the 5th European Conference on*, pages 1882–1885. IEEE, 2011.